A Novel Sin Model SMEx with Application on COVID-19 and Precipitation Data

Amani Alrumayh[1] and Hazar A. Khogeer[2,*]

[1] Department of Mathematics, College of Science, Northern Border University, Arar, 73311, Saudi Arabia

[2] Department of Mathematics, College of Science, Umm Al-Qura University, Makkah, 21955, Saudi Arabia

INFORMATION

Keywords:
Covid-19
inference
moment exponential distribution
moments
Sine-G family

DOI: 10.23967/j.rimni.2025.10.74217

Revista Internacional de Métodos Numéricos para Cálculo y Diseño en Ingeniería

A Novel Sin Model SMEx with Application on COVID-19 and Precipitation Data

Amani Alrumayh[1] **and Hazar A. Khogeer**[2,*]

[1]Department of Mathematics, College of Science, Northern Border University, Arar, 73311, Saudi Arabia

[2]Department of Mathematics, College of Science, Umm Al-Qura University, Makkah, 21955, Saudi Arabia

ABSTRACT

The present study proposes a new and flexible trigonometric extension of the moment exponential distribution, termed the Sine Moment Exponential (SMEx) distribution, developed using the sine-G family of distributions. This model offers an attractive alternative to well-known lifetime distributions by providing enhanced flexibility for analyzing lifetime datasets that exhibit leptokurtic or platykurtic behavior. Several statistical properties of the SMEx distribution are derived, including its moments, quantile function, mean residual life, and order statistics. To assess its performance, five different estimation approaches are applied, including Anderson-Darling estimation, maximum likelihood estimation, Cramer-von Mises estimation, ordinary least squares estimation, and weighted least squares estimation. A detailed Monte Carlo simulation study is utilized to illustrate the estimation behavior of these considered estimation procedures. In the end, two datasets associated with COVID-19 and precipitation are utilized to illustrate the applicability and flexibility of the proposed distribution. It is found that the proposed distribution efficiently analyzed these datasets as compared to competitive distributions.

OPEN ACCESS

Received: 06/10/2025

Accepted: 28/10/2025

Published: 23/01/2026

DOI
10.23967/j.rimni.2025.10.74217

Keywords:
Covid-19
inference
moment exponential distribution
moments
Sine-G family

1 Introduction

Data analysis has been a major area of research, particularly in probabilistic reasoning and measurement. Probability models play a vital role in various fields such as radiology, engineering, hydrology, epidemiology, risk management, industrial management, biological sciences, and medicine [1–3]. These probability models facilitate describing, modeling, and forecasting the time until an event of interest, such as system failure, illness remission, or product lifetime [4–8].

In literature, numerous classical distributions have been introduced to adequately represent the stochastic character of real-life occurrences. Unfortunately, the classical models are unable to represent a variety of events that occur today, although many of them require modeling. The existing probability distribution may constantly be improved by making it more adaptive or appropriate for certain real-world settings. For the generalization of baseline models, several approaches and techniques have been proposed for this purpose. These include, but are not limited to, transmuted-G [9], Beta-G [10], Weibull-G [11], Sine-G [12], Fréchet-G [13], Power Lindley-G [14], Burr X-G [15], Arctan-X [16], Teissier-G [17], Marshall–Olkin sine–G [18], Cosine Topp–Leone-G [19], Lambert-G [20],

*Correspondence: Hazar A. Khogeer (hakhogeer@uqu.edu.sa).

Tangent exponential-G [21], novel Sin-G [22], Bivariate weibull-g family [23], new shifted Lomax-X family [24], nitrosophic logic using the Gompertz family [25], exponentiated generalized alpha power family [26], Marshall-Olkin cosine Topp-Leone distribution family [27] and Cosine inverse Lomax-G family [28]. Each of these generalization techniques modified the baseline models through transformation, resulting in a more versatile class capable of analyzing a wide range of data patterns.

Recently, trigonometric-based extended models have garnered scholarly interest due to their mathematical tractability and flexibility. The sine-G family of distributions got great attention within the area of trigonometric generalized families. The probability density function (PDF) of the sine-G family is as follows:

$$f(x;\phi) = \frac{\pi}{2} g(x;\phi)\cos\left(\frac{\pi}{2} G(x;\phi)\right),\ x \in R, \tag{1}$$

where $G(x;\phi)$ is an arbitrary baseline cumulative distribution function (CDF) of any continuous probability distribution, which depends on a parameter vector ϕ. The CDF corresponding to PDF in Eq. (1) is as follows:

$$F(x;\phi) = \sin\left(\frac{\pi}{2} G(x;\phi)\right),\ x \in R. \tag{2}$$

The moment exponential distribution is the simplest distribution originally introduced [29] and has derived its main mathematical characteristics, such as moments, failure rate, moment generating function, skewness, and kurtosis. The PDF and CDF of the MEx distribution are given, respectively.

$$g(x;\eta) = \frac{x}{\eta^2} e^{-\frac{x}{\eta}},\ x > 0,\ \eta > 0, \tag{3}$$

and

$$G(x;\eta) = 1 - \left(1 + \frac{x}{\eta}\right) e^{-\frac{x}{\eta}}, \tag{4}$$

where η is a scale parameter.

The current study contributes to that ongoing effort by introducing an improved extension of the moment exponential (MEx) distribution, the SMEx distribution. The key objectives of the paper include:

- To introduce an improved MEx distribution using the Sine-G family of distributions. The new probability model is named the Sine Moment Exponential (SMEx) distribution. The SMEx distribution demonstrated a unimodal and positively skewed density function and increasing failure rate shapes.
- To derive and explore its various mathematical characteristics.
- Five different estimation approaches are utilized to estimate the SMEx distribution parameter. A detailed Monte Carlo simulation is also used to demonstrate the estimation performance of these estimation methods.
- The flexibility and applicability of the SMEx distribution are assessed utilizing two datasets related to epidemiological and climatic data.

The remainder of the study is planned as follows. The SMEx distribution is introduced in Section 2. We derived and discussed its key theoretical characteristics in Section 3. Five different estimation approaches are discussed in Section 4. A detailed simulation study is performed in Section 5. Two different datasets are analyzed in Section 6, and concluding remarks are provided in Section 7.

2 Derivation of SMEx Distribution

A non-negative random variable follows the SMEx distribution with one parameter η can be derived by using Eqs. (3) and (4) into Eqs. (1) and (2).

The PDF and CDF of the SMEx distribution are given in Eqs. (5) and (6), respectively.

$$F(x;\,\eta) = sin\left[\frac{\pi}{2}\left(1-\left(1+\frac{x}{\eta}\right)e^{-\frac{x}{\eta}}\right)\right],\ \eta>0,\ x>0, \tag{5}$$

and

$$f(x;\,\eta) = \frac{\pi}{2}\frac{x}{\eta^2}e^{-\frac{x}{\eta}}cos\left[\frac{\pi}{2}\left(1-\left(1+\frac{x}{\eta}\right)e^{-\frac{x}{\eta}}\right)\right]. \tag{6}$$

The reliability function of the SMEx distribution is

$$S(x;\,\eta) = 1-sin\left[\frac{\pi}{2}\left(1-\left(1+\frac{x}{\eta}\right)e^{-\frac{x}{\eta}}\right)\right]. \tag{7}$$

The failure rate of the SMEx distribution is given by

$$h(x;\,\eta) = \frac{\pi x e^{-\frac{x}{\eta}}cos\left[\frac{\pi}{2}\left(1-\left(1+\frac{x}{\eta}\right)e^{-\frac{x}{\eta}}\right)\right]}{2\eta^2\left\{1-sin\left[\frac{\pi}{2}\left(1-\left(1+\frac{x}{\eta}\right)e^{-\frac{x}{\eta}}\right)\right]\right\}}. \tag{8}$$

The reversed hazard function $rh(x;\,\eta)$ is

$$rh(x;\,\eta) = \frac{\frac{\pi}{2}\frac{x}{\eta^2}e^{-\frac{x}{\eta}}cos\left[\frac{\pi}{2}\left(1-\left(1+\frac{x}{\eta}\right)e^{-\frac{x}{\eta}}\right)\right]}{sin\left[\frac{\pi}{2}\left(1-\left(1+\frac{x}{\eta}\right)e^{-\frac{x}{\eta}}\right)\right]}. \tag{9}$$

The plots of PDF and failure rate for some choices of parameter η are illustrated in Fig. 1.

For lower parameter values (e.g., $\eta = 0.5,\ 0.8$) the PDF of SMEx distribution is highly concentrated near to origin with sharp peaks, which depicts that the SMEx distribution places most of its mass near zero. As the parameter increases, the peak of the density shifts to the right side and becomes flatter, indicating more dispersion in the data.

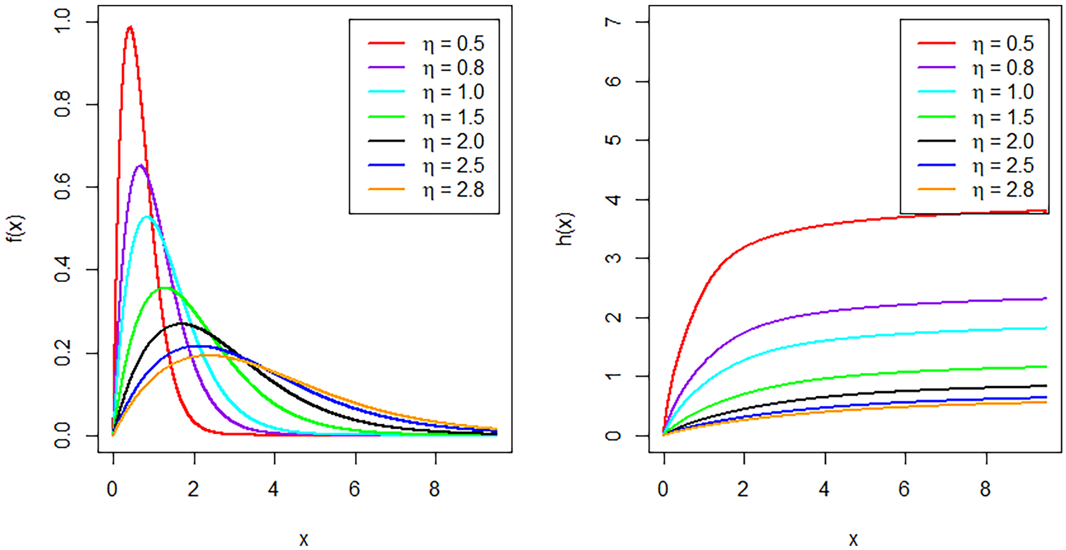

Figure 1: Density and hazard function curves of SMEx distribution based on different values of η

The failure rate begins high and decreases rapidly for lower η values, indicating a decreasing failure rate behavior. This indicates early failures are more likely, which then decline over time. For moderate to higher parameter choices of the SMEx distribution, the failure rate exhibits non-monotonic behavior. These failure rate behaviors make the SMEx distribution flexible for analysis of reliability and survival data, since it can capture early life failures, constant risks, or wear-out behavior depending on the choice of parameter η.

3 Theoretical Characteristics of SMEx Distribution

In this section, we compute and explore some key statistical properties of SMEx distribution.

3.1 Important Series

In this section, we present the alternative form of the density function of the SMEx distribution. Using this density, the properties of the SMEx distribution can be easily derived. Eq. (6) can be rewritten as

$$f(x;\eta) = \frac{\pi}{2}\frac{x}{\eta^2}e^{-\frac{x}{\eta}} cos\left[\frac{\pi}{2}\left(1-\left(1+\frac{x}{\eta}\right)e^{-\frac{x}{\eta}}\right)\right].$$

By using the series of the Cos function, i.e., $\cos[P] = \sum_{i=0}^{\infty}\frac{(-1)^i}{(2i)!}P^{2i}$, the $f(x;\ \eta)$ can be rewritten as

$$f(x;\ \eta) = \frac{\pi}{2}\frac{x}{\eta^2}e^{-\frac{x}{\eta}}\sum_{i=0}^{\infty}\frac{(-1)^i}{(2i)!}\left(\frac{\pi}{2}\left(1-\left(1+\frac{x}{\eta}\right)e^{-\frac{x}{\eta}}\right)\right)^{2i},$$

$$f\left(x;\eta\right)=\sum_{i=0}^{\infty}\frac{\left(-1\right)^{i}}{\left(2i\right)!}\left(\frac{\pi}{2}\right)^{2i+1}\frac{x}{\eta^{2}}e^{-\frac{x}{\eta}}\left(1-\left(1+\frac{x}{\eta}\right)e^{-\frac{x}{\eta}}\right)^{2i}. \quad (10)$$

By applying the binomial expansion $(1-Q)^{2i}=\sum_{j=0}^{2i}(-1)^{j}\binom{2i}{j}Q^{j}$ to Eq. (10), we have

$$f\left(x;\eta\right)=\sum_{i=0}^{\infty}\sum_{j=0}^{2i}\frac{\left(-1\right)^{i+j}}{\left(2i\right)!}\left(\frac{\pi}{2}\right)^{2i+1}\binom{2i}{j}\frac{x}{\eta^{2}}e^{-\frac{x}{\eta}(j+1)}\left(1+\frac{x}{\eta}\right)^{j}. \quad (11)$$

Again, by applying the binomial *expansion* $(1+x)^{k}=\sum_{s=0}^{k}\binom{k}{s}x^{s}$ to Eq. (11), we obtain

$$f\left(x;\eta\right)=\sum_{i=0}^{\infty}\sum_{j=0}^{2i}\sum_{k=0}^{j}\frac{\left(-1\right)^{i+j}\left(\frac{\pi}{2}\right)^{2i+1}}{k!\left(2i-j\right)!\left(j-k\right)\eta^{2+k}}x^{k+1}e^{-\frac{x}{\eta}(j+1)},$$

$$f\left(x;\eta\right)=\sum_{i=0}^{\infty}\sum_{j=0}^{2i}\sum_{k=0}^{j}\vartheta_{i,j,k}x^{k+1}e^{-\frac{x}{\eta}(j+1)}, \quad (12)$$

where

$$\vartheta_{i,j,k}=\frac{\left(-1\right)^{i+j}\left(\frac{\pi}{2}\right)^{2i+1}}{k!\left(2i-j\right)!\left(j-k\right)\eta^{2+k}}.$$

3.2 Incomplete Moments

The nth incomplete moment of the SMEx distribution can be derived from Eq. (12) as follows:

$$\rho_{n}=\int_{0}^{z}x^{n}f\left(x;\ \eta\right)dx,$$

$$\rho_{n}=\sum_{i=0}^{\infty}\sum_{j=0}^{2i}\sum_{k=0}^{j}\vartheta_{i,j,k}\int_{0}^{z}x^{n+k+1}e^{-\frac{x}{\eta}(j+1)}dx.$$

Now transform $v=\frac{x(j+1)}{\eta}$, we have

$$\rho_{n}=\sum_{i=0}^{\infty}\sum_{j=0}^{2i}\sum_{k=0}^{j}\vartheta_{i,j,k}\int_{0}^{\frac{z(j+1)}{\eta}}\left(\frac{\eta v}{j+1}\right)^{n+k+1}e^{-v}\frac{\eta}{\left(j+1\right)}dv,$$

$$\rho_{n}=\sum_{i=0}^{\infty}\sum_{j=0}^{2i}\sum_{k=0}^{j}\vartheta_{i,j,k}\left(\frac{\eta}{j+1}\right)^{n+k+2}\int_{0}^{\frac{z(j+1)}{\eta}}v^{n+k+1}e^{-v}dv.$$

The final expression is

$$\rho_{n}=\sum_{i=0}^{\infty}\sum_{j=0}^{2i}\sum_{k=0}^{j}\vartheta_{i,j,k}\left(\frac{\eta}{j+1}\right)^{n+k+2}\gamma\left(\left(n+k+2\right),\ \frac{z\left(j+1\right)}{\eta}\right),\ \eta>0,\ z>0, \quad (13)$$

where $\gamma\left(r,\ a\right)=\int_{0}^{a}v^{r-1}e^{-v}dv$ is the lower incomplete gamma function.

3.3 Moments with Associated Measures

The r-th moment about the origin of the SMEx distribution can be computed from the Eq. (12) as follows.

$$\mu_r^{'} = \sum_{i=0}^{\infty}\sum_{j=0}^{2i}\sum_{k=0}^{j}\vartheta_{i,j,k}\int_0^{\infty} x^{r+k+1} e^{-\frac{x}{\eta}(j+1)} dx. \tag{14}$$

Now use the definition of the gamma function.

$$\int_0^{\infty} x^{a-1} e^{-\frac{x}{b}} dx = \Gamma(a)\, b^a,\ for\ a > 0,\ b > 0.$$

So for:

$$\int_0^{\infty} x^{r+k+1} e^{-\frac{x}{\eta}(j+1)} dx = \Gamma(r+k+2)\,(\eta\,(j+1))^{r+k+2}.$$

Substitute into the Eq. (15)

$$\mu_r^{'} = \sum_{i=0}^{\infty}\sum_{j=0}^{2i}\sum_{k=0}^{j}\vartheta_{i,j,k}\Gamma(r+k+2)\,(\eta\,(j+1))^{r+k+2}. \tag{15}$$

Consequently, the mean, standard deviation (SD), coefficients of skewness (CS), and kurtosis (CK) of X can be expressed as

$$\mu = \sum_{i=0}^{\infty}\sum_{j=0}^{2i}\sum_{k=0}^{j}\frac{(-1)^{i+j}\left(\frac{\pi}{2}\right)^{2i+1}}{k!\,(2i-j)\,!\,(j-k)\,\eta^{2+k}}\Gamma(k+3)\,(\eta\,(j+1))^{k+3},$$

$$SD(X) = \sqrt{\mu_2 - (\mu_1)^2},$$

$$CS(X) = \frac{\mu_3 - 3\mu_2 + 2\mu_1^3}{\left(\mu_2 - (\mu_1)^2\right)^{1.5}},$$

and

$$CK(X) = \frac{\mu_4 - 4\mu_3 + 6\mu_2(\mu_1)^2 - 3(\mu_1)^4}{\left(\mu_2 - (\mu_1)^2\right)^2}.$$

Table 1 compiles some key statistical measures of the SMEx distribution, showcasing various choices of parameter η. These measures reveal interesting trends with changes in parameter η. The average value of the SMEx distribution demonstrations a declining pattern with an increase in parameter η. Similarly, SD shows a decreasing trend. The coefficient of skewness (CS) upsurge with higher values of the η parameter demonstrating that the models shape shifts from being moderately skewed to right side and becomes highly right-skewed as parameter η grows. Correspondingly, the coefficient of kurtosis (CK) also rises with higher values of parameter η, suggesting that the distribution tails become heavier and the data distribution exhibits greater peakedness and more extreme values at higher levels of parameter η.

Table 1: Numerical values of different statistical measures of the SMEx distribution

η	Mean	$E(X^2)$	$E(X^3)$	$E(X^4)$	SD	CV	CS	CK
0.3	0.3132	0.1632	0.1009	0.0695	0.2550	0.8142	0.5435	2.4413
0.5	0.3798	0.2396	0.1704	0.1305	0.3089	0.8134	0.2353	1.8201
0.8	0.2981	0.2049	0.1545	0.1234	0.3406	1.1424	0.6143	1.8376
1.0	0.2381	0.1674	0.1283	0.1036	0.3328	1.3976	0.9678	2.3459
1.5	0.1399	0.1009	0.0787	0.0644	0.2853	2.0396	1.8013	4.6895
2.0	0.0898	0.0655	0.0515	0.0423	0.2397	2.6700	2.5609	8.1265
2.5	0.0620	0.0456	0.0359	0.0296	0.2042	3.2912	3.2791	12.494
3.0	0.0453	0.0334	0.0264	0.0218	0.1771	3.9063	3.9738	17.744
3.5	0.0345	0.0255	0.0202	0.0167	0.1559	4.5175	4.6539	23.861
4.0	0.0271	0.0201	0.0159	0.0132	0.1391	5.1258	5.3245	30.836
4.5	0.0219	0.0162	0.0129	0.0107	0.1255	5.7323	5.9884	38.667
5.0	0.0180	0.0134	0.0106	0.0088	0.1143	6.3372	6.6476	47.350
5.5	0.0151	0.0112	0.0089	0.0074	0.1049	6.9411	7.3032	56.885
6.0	0.0128	0.0095	0.0076	0.0063	0.0969	7.5442	7.9561	67.270
6.5	0.0110	0.0082	0.0065	0.0054	0.0900	8.1466	8.6069	78.505
7.0	0.0096	0.0072	0.0057	0.0047	0.0840	8.7485	9.2560	90.590

3.4 Mean Residual Life (MRL)

The MRL at time t is defined as:

$$m(t) = \mathbb{E}[X - t | X > t] = \frac{1}{S(t)} \int_t^\infty (x - t) f(x; \eta)\, dx = \frac{1}{S(t)} \left[\int_t^\infty x f(x; \eta)\, dx - t \right].$$

Now using the PDF given in Eq. (12)

$$m(t) = \frac{1}{S(t)} \left[\sum_{i=0}^{\infty} \sum_{j=0}^{2i} \sum_{k=0}^{j} \vartheta_{i,j,k} \int_t^\infty x^{k+2} e^{-\frac{x}{\eta}(j+1)} dx - t \right]. \tag{16}$$

Now compute

$$\int_t^\infty x^{k+2} e^{-\frac{x}{\eta}(j+1)} dx = \left(\frac{\eta}{j+1} \right)^{k+2} \gamma \left((k+3), \frac{t(j+1)}{\eta} \right).$$

The final form of MRL is

$$m(t) = \frac{1}{\left(1 - sin\left[\frac{\pi}{2}\left(1 - \left(1 + \frac{t}{\eta}\right) e^{-\frac{t}{\eta}}\right)\right]\right)} \left[\sum_{i=0}^{\infty} \sum_{j=0}^{2i} \sum_{k=0}^{j} \vartheta_{i,j,k} \left(\frac{\eta}{j+1} \right)^{k+2} \gamma \left((k+3), \frac{t(j+1)}{\eta} \right) - t \right].$$

3.5 Quantile Function

The quantile function is defined as the function that gives the value below which a given proportion of data falls. If $F(x)$ is the CDF of a random variable X, the quantile function $Q(p)$ is its inverse, defined as:

$\mathrm{Q}(P) = F^{-1}(p)\,,\ 0 \leq p \leq 1.$

Set $p = G(x)$

$$p = \sin\left[\frac{\pi}{2}\left(1 - \left(1 + \frac{x}{\eta}\right)e^{-\frac{x}{\eta}}\right)\right].$$

Take archsin on both sides.

$$\sin^{-1}(p) = \frac{\pi}{2}\left(1 - \left(1 + \frac{x}{\eta}\right)e^{-\frac{x}{\eta}}\right).$$

Now solve the exponential term.

$$\left(\frac{2}{\pi}\right)\sin^{-1}(p) = 1 - \left(1 + \frac{x}{\eta}\right)e^{-\frac{x}{\eta}},$$
$$1 - \frac{2}{\pi}\sin^{-1}(p) = \left(1 + \frac{x}{\eta}\right)e^{-\frac{x}{\eta}}.$$

Let $y = 1 - \frac{2}{\pi}\sin^{-1}(p)$, so $\left(1 + \frac{x}{\eta}\right)e^{-\frac{x}{\eta}} = y$.

Consider $z = -\frac{x}{\eta} \implies x - \eta z$, then $(1 - z)\,e^{z} = y$. Now multiply both sides by e^{-1}, we get $(1 - z)\,e^{z-1} = ye^{-1}$.

Now defined $w = 1 - z$, so $we^{-(w-1)} = ye^{-1} \implies we^{-w} = -ye^{-1}$. So $w = W\left(-ye^{-1}\right)$.

Now back-substitute:

$$1 - z = W\left(-ye^{-1}\right) \implies z = 1 - W\left(-ye^{-1}\right),$$

Since $x = -\eta z$, we get $x = -\eta\left(1 - W\left(-ye^{-1}\right)\right) = \eta\left(W\left(-ye^{-1}\right) - 1\right)$. Now recall $y = 1 - \frac{2}{\pi}\sin^{-1}(p)$, so

$$Q(P) = -\eta\left[W\left(-\left(1 - \left(\frac{2}{\pi}\right)\sin^{-1}(p)\right)e^{-1}\right) + 1\right]. \tag{17}$$

3.6 Order Statistics

Let the random variable X follow SMEx distribution and $x_{(1)}, x_{(2)}, \ldots, x_{(n)}$ represents the order statistics. The r-th order statistics from a sample of size n is

$$f(X_{r:n}) = \frac{n!}{(r-1)!\,(n-r)!}\left(F(x)\right)^{r-1}\left(1 - F(x)\right)^{n-r} f(x)$$

Substituting the PDF and CDF of SMEx distribution

$$f(X_{r:n}) = \frac{n!\,\pi x e^{-\frac{x}{\eta}}}{2\eta^2\,(r-1)!\,(n-r)!}\left\{sin\left[\frac{\pi}{2}\left(1 - \left(1 + \frac{x}{\eta}\right)e^{-\frac{x}{\eta}}\right)\right]\right\}^{r-1}$$
$$\times\left\{1 - sin\left[\frac{\pi}{2}\left(1 - \left(1 + \frac{x}{\eta}\right)e^{-\frac{x}{\eta}}\right)\right]\right\}^{n-r} \times cos\left[\frac{\pi}{2}\left(1 - \left(1 + \frac{x}{\eta}\right)e^{-\frac{x}{\eta}}\right)\right].$$

The densities of minimum and maximum order statistics are

$$f\left(X_{1:n}\right) = n\left\{1 - sin\left[\frac{\pi}{2}\left(1 - \left(1 + \frac{x}{\eta}\right)e^{-\frac{x}{\eta}}\right)\right]\right\}^{n-1} \times \frac{\pi}{2}\frac{x}{\eta^2}e^{-\frac{x}{\eta}}cos\left[\frac{\pi}{2}\left(1 - \left(1 + \frac{x}{\eta}\right)e^{-\frac{x}{\eta}}\right)\right],$$

and

$$f\left(X_{n:n}\right) = n\left\{sin\left[\frac{\pi}{2}\left(1 - \left(1 + \frac{x}{\eta}\right)e^{-\frac{x}{\eta}}\right)\right]\right\}^{n-1} \times \frac{\pi}{2}\frac{x}{\eta^2}e^{-\frac{x}{\eta}}cos\left[\frac{\pi}{2}\left(1 - \left(1 + \frac{x}{\eta}\right)e^{-\frac{x}{\eta}}\right)\right].$$

4 Parameter Estimation

In this section, the parameters of the SMEx distribution are estimated using different estimation approaches. The considered estimation techniques are the maximum likelihood estimation (MLE), Ordinary Least Squares estimation (OLSE), Anderson-Darling estimation (ADE), Weighted Least Squares (WLSE), and Cramer-von Mises estimation (CVME). For more information on the implementation of estimation methods, see [30–34].

4.1 Maximum Likelihood Estimation

The MLE technique is extensively preferred due to its desirable estimation properties, together with consistency, invariance, and asymptotic efficiency. The MLE involves maximizing the log-likelihood function to obtain the estimators. Consider a random sample $(x_1, x_2, \ldots, x_n)$ of size n taken from the SMEx distribution. The log-likelihood $l(\eta)$ for the SMEx distribution is given by

$$l(\eta) = n\log\left(\frac{\pi}{2}\right) - 2n\log(\eta) + \sum_{i=1}^{n}\log(x_i) - \sum_{i=1}^{n}\frac{x_i}{\eta} + \sum_{i=1}^{n}\log\left(\cos\left(\frac{\pi}{2}\left(1 - \left(1 + \frac{x_i}{\eta}\right)e^{-\frac{x_i}{\eta}}\right)\right)\right).$$

Suppose $\hat{\eta}$ is the MLE of the parameter η. It is obtained by solving the nonlinear equation.

$$\frac{\partial l(\eta)}{\partial \eta} = \sum_{i=1}^{n}\frac{x_i}{\eta^2} - \frac{2n}{\eta} + \sum_{i=1}^{n}\left[\left(\frac{\pi}{2}\right)\frac{x^2}{\eta^3}e^{-\frac{x}{\eta}}\tan\left(\frac{\pi}{2}\left(1 - \left(1 + \frac{x_i}{\eta}\right)e^{-\frac{x_i}{\eta}}\right)\right)\right].$$

4.2 Ordinary Least Squares Estimation

The OLSE is often utilized to estimate the parameters in linear models. Consider $x_{1:n}, x_{2:n}, \ldots, x_{n:n}$ represent the order statistics from a random sample of size n taken from the SMEx distribution. To obtain the OLSE of the parameter η of the SMEx distribution, the distance below is minimized.

$$O^* = \sum_{i=1}^{n}\left[\sin\left(\frac{\pi}{2}\left(1 - \left(1 + \frac{x_{i:n}}{\eta}\right)e^{-\frac{x_{i:n}}{\eta}}\right)\right) - \frac{i}{n+1}\right]^2.$$

4.3 Anderson-Darling Estimation

The Anderson-Darling (AD) statistic is a goodness-of-fit measure that evaluates the discrepancy between an empirical CDF and its theoretical counterpart. It is a type of minimal distance estimation in which model parameters are estimated by reducing this discrepancy. Consider $x_{1:n}, x_{2:n}, \ldots, x_{n:n}$ represent the order statistics from a random sample of size n taken from the SMEx distribution. The ADE of parameter η is derived by minimizing the following statistic.

$$A^* = -n - \frac{1}{n}\sum_{i=1}^{n}(2i-1)\left\{\log\left(\sin\left(\frac{\pi}{2}\left(1-\left(1+\frac{x_{i:n}}{\eta}\right)e^{-\frac{x_{i:n}}{\eta}}\right)\right)\right)\right.$$
$$\left.+\log\left(1-\sin\left(\frac{\pi}{2}\left(1-\left(1+\frac{x_{i:n}}{\eta}\right)e^{-\frac{x_{i:n}}{\eta}}\right)\right)\right)\right\}.$$

4.4 Cramer-Von Mises Estimation

The CVME approach is another commonly utilized goodness-of-fit-based estimator, which is derived from the CVM statistic. Let $x_{1:n}, x_{2:n}, \ldots, x_{n:n}$ represent the order statistics from a random sample of size n taken from the SMEx distribution. The CVME of parameter η is derived by minimizing the following statistic.

$$C^* = \frac{1}{12n} + \sum_{i=1}^{n}\left[\sin\left(\frac{\pi}{2}\left(1-\left(1+\frac{x_{i:n}}{\eta}\right)e^{-\frac{x_{i:n}}{\eta}}\right)\right) - \frac{2i-1}{2n}\right]^2.$$

4.5 Weighted Ordinary Least Squares Estimation

Consider $x_{1:n}, x_{2:n}, \ldots, x_{n:n}$ represent the order statistics from a random sample of size n taken from the SMEx distribution. To obtain the OLSE of the parameter η of the SMEx distribution, the distance below is minimized.

$$W^* = \sum_{i=1}^{n}\left[\frac{(n+1)^2(n+2)}{(n+1-i)\,i}\right]\left[\sin\left(\frac{\pi}{2}\left(1-\left(1+\frac{x_{i:n}}{\eta}\right)e^{-\frac{x_{i:n}}{\eta}}\right)\right) - \frac{i}{n+1}\right]^2.$$

5 Simulation Study

This section presents the findings of a detailed Monte Carlo simulation study to evaluate the performance of the estimation approaches derived. The random samples are generated from the SMEx distribution using Eq. (17) of size $n = 25, 50, 75, 100, 150$, and 200. The estimation process is repeated for N = 10,000 times for each sample and choice of parameter. We compute average estimate (AE), absolute bias (AB), mean relative error (MRE), and mean squared error (MSE). The corresponding formulas for these performance metrics are

$$AB(\hat{n}) = \frac{1}{10000}\sum_{i=1}^{10000}\left|\hat{n}-n\right|, MRE(\hat{n}) = \frac{1}{10000}\sum_{i=1}^{10000}\frac{\left|\hat{n}-n\right|}{n}, \text{and } MSE(\hat{n}) = \frac{1}{10000}\sum_{i=1}^{10000}(\hat{n}-n)^2.$$

Six different parameter settings for η are considered: 0.5, 1.0, 2.0, 3.0, 4.0, and 5.0. The corresponding simulation results are presented in Tables 2–8.

Table 2: Estimates, AB, MRE, MSE, considering parameter $\eta = 0.5$ and different sample sizes

Estimate	n	ML	A^*	C^*	O^*	W^*
AE	25	0.49903	0.50292	0.50353	0.50520	0.50337
	50	0.50023	0.50283	0.50071	0.50099	0.50282
	75	0.49969	0.50089	0.50086	0.50101	0.50129
	100	0.49972	0.50106	0.50077	0.50112	0.50134
	150	0.50013	0.50053	0.50043	0.50038	0.50058
	200	0.49988	0.50035	0.50040	0.50005	0.50037
AB	25	0.00097	0.00292	0.00353	0.00520	0.00337
	50	0.00023	0.00283	0.00071	0.00099	0.00282
	75	0.00031	0.00089	0.00086	0.00101	0.00129
	100	0.00028	0.00106	0.00077	0.00112	0.00134
	150	0.00013	0.00053	0.00043	0.00038	0.00058
	200	0.00012	0.00035	0.00040	0.00005	0.00037
MRE	25	0.00194	0.00584	0.00705	0.01040	0.00674
	50	0.00045	0.00566	0.00142	0.00198	0.00565
	75	0.00063	0.00178	0.00172	0.00202	0.00258
	100	0.00056	0.00211	0.00154	0.00225	0.00268
	150	0.00027	0.00107	0.00086	0.00077	0.00116
	200	0.00025	0.00071	0.00080	0.00011	0.00074
MSE	25	0.00396	0.00441	0.00487	0.00511	0.00460
	50	0.00198	0.00220	0.00245	0.00243	0.00227
	75	0.00130	0.00152	0.00159	0.00165	0.00152
	100	0.00100	0.00113	0.00120	0.00119	0.00112
	150	0.00067	0.00074	0.00081	0.00080	0.00075
	200	0.00049	0.00056	0.00058	0.00058	0.00056

Table 3: Estimates, AB, MRE, MSE, considering parameter $\eta = 1.0$ and different sample sizes

Estimate	n	ML	A^*	C^*	O^*	W^*
AE	25	0.99719	1.00818	1.00282	1.00822	1.00903
	50	0.99801	1.00450	1.00272	1.00534	1.00470
	75	0.99958	1.00338	1.00221	1.00265	1.00239
	100	0.99910	1.00146	1.00065	1.00011	1.00201
	150	0.99897	1.00141	1.00213	1.00162	1.00074
	200	1.00010	1.00071	1.00014	1.00060	1.00206

(Continued)

Table 3 (continued)

Estimate	n	ML	A^*	C^*	O^*	W^*
AB	25	0.00281	0.00818	0.00282	0.00822	0.00903
	50	0.00199	0.00450	0.00272	0.00534	0.00470
	75	0.00042	0.00338	0.00221	0.00265	0.00239
	100	0.00090	0.00146	0.00065	0.00011	0.00201
	150	0.00103	0.00141	0.00213	0.00162	0.00074
	200	0.00010	0.00071	0.00014	0.00060	0.00206
MRE	25	0.00281	0.00818	0.00282	0.00822	0.00903
	50	0.00199	0.00450	0.00272	0.00534	0.00470
	75	0.00042	0.00338	0.00221	0.00265	0.00239
	100	0.00090	0.00146	0.00065	0.00011	0.00201
	150	0.00103	0.00141	0.00213	0.00162	0.00074
	200	0.00010	0.00071	0.00014	0.00060	0.00206
MSE	25	0.01590	0.01759	0.01934	0.01961	0.01838
	50	0.00778	0.00884	0.00964	0.00973	0.00931
	75	0.00532	0.00597	0.00651	0.00656	0.00595
	100	0.00395	0.00439	0.00470	0.00486	0.00441
	150	0.00260	0.00298	0.00325	0.00322	0.00293
	200	0.00202	0.00213	0.00233	0.00236	0.00229

Table 4: Estimates, AB, MRE, MSE, considering parameter $\eta = 1.5$ and different sample sizes

Estimate	n	ML	A^*	C^*	O^*	W^*
AE	25	1.51035	1.51360	1.51035	1.51379	1.51462
	50	1.50484	1.50591	1.50484	1.50714	1.50494
	75	1.50222	1.50524	1.50222	1.50502	1.50319
	100	1.50360	1.50284	1.50360	1.50291	1.50427
	150	1.50070	1.50188	1.50070	1.50099	1.50089
	200	1.50100	1.50082	1.50100	1.50211	1.50104
AB	25	0.01035	0.01360	0.01035	0.01379	0.01462
	50	0.00484	0.00591	0.00484	0.00714	0.00494
	75	0.00222	0.00524	0.00222	0.00502	0.00319
	100	0.00360	0.00284	0.00360	0.00291	0.00427
	150	0.00070	0.00188	0.00070	0.00099	0.00089
	200	0.00100	0.00082	0.00100	0.00211	0.00104
MRE	25	0.00690	0.00906	0.00690	0.00919	0.00975
	50	0.00323	0.00394	0.00323	0.00476	0.00329
	75	0.00148	0.00349	0.00148	0.00335	0.00213
	100	0.00240	0.00190	0.00240	0.00194	0.00284
	150	0.00047	0.00125	0.00047	0.00066	0.00059
	200	0.00067	0.00055	0.00067	0.00140	0.00070

(Continued)

Table 4 (continued)

Estimate	n	ML	A^*	C^*	O^*	W^*
MSE	25	0.04402	0.04159	0.04402	0.04364	0.04223
	50	0.02140	0.02014	0.02140	0.02221	0.02098
	75	0.01455	0.01338	0.01455	0.01482	0.01329
	100	0.01093	0.00978	0.01093	0.01093	0.01014
	150	0.00722	0.00667	0.00722	0.00734	0.00665
	200	0.00548	0.00502	0.00548	0.00557	0.00507

Table 5: Estimates, AB, MRE, MSE considering parameter $\eta = 2.0$ and different sample sizes

Estimate	n	ML	A^*	C^*	O^*	W^*
AE	25	1.99322	2.01527	2.01119	2.01498	2.02364
	50	1.99871	2.00579	2.00679	2.00876	2.01050
	75	1.99965	2.00732	2.00266	2.00676	2.00566
	100	2.00064	2.00455	2.00188	2.00492	2.00372
	150	1.99907	2.00421	2.00146	2.00436	2.00234
	200	2.00036	2.00125	2.00073	2.00213	2.00257
AB	25	0.00678	0.01527	0.01119	0.01498	0.02364
	50	0.00129	0.00579	0.00679	0.00876	0.01050
	75	0.00035	0.00732	0.00266	0.00676	0.00566
	100	0.00064	0.00455	0.00188	0.00492	0.00372
	150	0.00093	0.00421	0.00146	0.00436	0.00234
	200	0.00036	0.00125	0.00073	0.00213	0.00257
MRE	25	0.00339	0.00764	0.00559	0.00749	0.01182
	50	0.00064	0.00289	0.00339	0.00438	0.00525
	75	0.00017	0.00366	0.00133	0.00338	0.00283
	100	0.00032	0.00228	0.00094	0.00246	0.00186
	150	0.00046	0.00211	0.00073	0.00218	0.00117
	200	0.00018	0.00062	0.00037	0.00107	0.00128
MSE	25	0.06259	0.07148	0.07987	0.08044	0.07516
	50	0.03170	0.03591	0.03866	0.03804	0.03726
	75	0.02116	0.02426	0.02616	0.02589	0.02409
	100	0.01606	0.01798	0.01908	0.01943	0.01763
	150	0.01058	0.01165	0.01312	0.01322	0.01173
	200	0.00805	0.00897	0.00949	0.00956	0.00906

Table 6: Estimates, AB, MRE, MSE, considering parameter $\eta = 3.0$ and different sample sizes

Estimate	n	ML	A^*	C^*	O^*	W^*
AE	25	2.99456	3.02127	3.01835	3.01934	3.03996
	50	2.99440	3.01139	3.00398	3.01371	3.01634
	75	2.99768	3.00524	3.00634	3.01137	3.00698
	100	2.99789	3.00343	3.00412	3.00495	3.00658
	150	2.99610	3.00599	3.00436	3.00425	3.00238
	200	3.00124	3.00388	3.00373	3.00270	3.00375
AB	25	0.00544	0.02127	0.01835	0.01934	0.03996
	50	0.00560	0.01139	0.00398	0.01371	0.01634
	75	0.00232	0.00524	0.00634	0.01137	0.00698
	100	0.00211	0.00343	0.00412	0.00495	0.00658
	150	0.00390	0.00599	0.00436	0.00425	0.00238
	200	0.00124	0.00388	0.00373	0.00270	0.00375
MRE	25	0.00181	0.00709	0.00612	0.00645	0.01332
	50	0.00187	0.00380	0.00133	0.00457	0.00545
	75	0.00077	0.00175	0.00211	0.00379	0.00233
	100	0.00070	0.00114	0.00137	0.00165	0.00219
	150	0.00130	0.00200	0.00145	0.00142	0.00079
	200	0.00041	0.00129	0.00124	0.00090	0.00125
MSE	25	0.14359	0.16260	0.17579	0.17770	0.17191
	50	0.07204	0.07874	0.08627	0.08843	0.08313
	75	0.04850	0.05323	0.05656	0.05834	0.05359
	100	0.03555	0.04014	0.04363	0.04325	0.04033
	150	0.02382	0.02678	0.02938	0.02897	0.02662
	200	0.01790	0.01971	0.02212	0.02167	0.02016

Table 7: Estimates, AB, MRE, MSE, considering parameter $\eta = 4.0$ and different sample sizes

Estimate	n	ML	A^*	C^*	O^*	W^*
AE	25	3.99148	4.03346	4.02214	4.03889	4.03123
	50	3.99603	4.01303	4.01361	4.02279	4.01234
	75	3.99520	4.01575	4.00745	4.00479	4.01004
	100	3.99442	4.00714	4.00618	4.00807	4.01195
	150	3.99542	4.00620	4.00818	4.01130	4.00635
	200	4.00095	4.00499	4.00273	4.00595	4.00539

(Continued)

Table 7 (continued)

Estimate	n	ML	A^*	C^*	O^*	W^*
AB	25	0.00852	0.03346	0.02214	0.03889	0.03123
	50	0.00397	0.01303	0.01361	0.02279	0.01234
	75	0.00480	0.01575	0.00745	0.00479	0.01004
	100	0.00558	0.00714	0.00618	0.00807	0.01195
	150	0.00458	0.00620	0.00818	0.01130	0.00635
	200	0.00095	0.00499	0.00273	0.00595	0.00539
MRE	25	0.00213	0.00837	0.00553	0.00972	0.00781
	50	0.00099	0.00326	0.00340	0.00570	0.00309
	75	0.00120	0.00394	0.00186	0.00120	0.00251
	100	0.00140	0.00179	0.00154	0.00202	0.00299
	150	0.00115	0.00155	0.00205	0.00283	0.00159
	200	0.00024	0.00125	0.00068	0.00149	0.00135
MSE	25	0.25473	0.28599	0.31216	0.31699	0.29633
	50	0.12853	0.14026	0.15496	0.15944	0.14146
	75	0.08462	0.09690	0.10403	0.10280	0.09589
	100	0.06562	0.07093	0.07800	0.07904	0.07443
	150	0.04219	0.04678	0.05197	0.05028	0.04785
	200	0.03177	0.03634	0.03922	0.03856	0.03519

Table 8: Performance summary by estimation method

Estimator	Small n performance	Large n performance	Bias trend	MSE trend	Overall rank
ML	Excellent (lowest AB, MSE)	Excellent (best overall)	Low	Low	1st
C*	Good	Very good	Low	Low	2nd
O*	Moderate	Good	Moderate	Moderate	3rd–4th
A*	Weak	Fair	Higher bias	Higher MSE	4th–5th
W*	Weak (esp. small n)	Fair to Moderate	Higher	Higher	5th

It is evident from Tables 2–8 and Fig. 2:

- The average estimate values across all five estimation approaches converge towards the true parameter value as the sample size rises.
- The ML estimation approach generally provides the closest estimates for all choices of η and n, particularly in smaller samples.
- The A^* (Anderson Darling) often shows higher absolute bias and mean relative error, especially for smaller sample sizes.
- The C^* (Cramer von Mises) tends to slightly overestimate across multiple settings, evident in its higher values of absolute bias and mean relative error for small sample sizes.

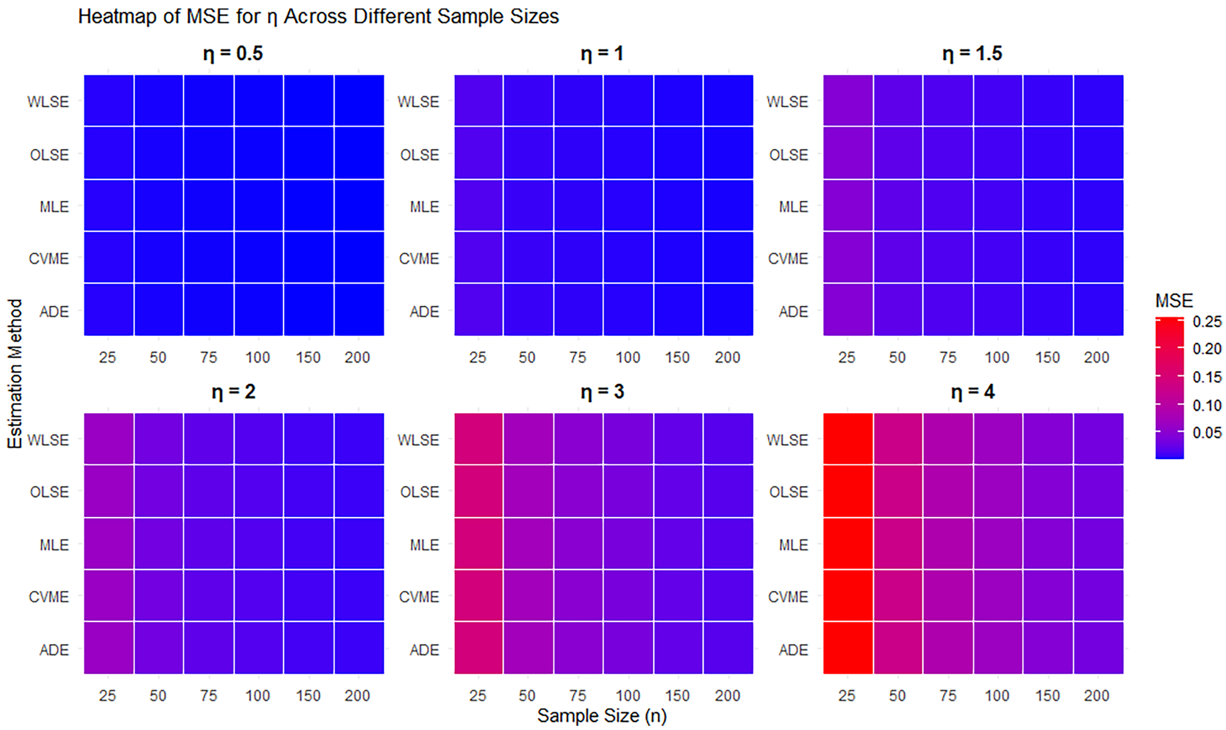

Figure 2: MSE heatmap for the parameter η under different estimators and sample sizes

6 Application of SMEx Distribution

In this section, we illustrate the applicability, flexibility, and potentiality of the proposed SMEx distribution by analyzing two datasets from different fields. For a detailed comparison, we apply the proposed distribution to both datasets along with considered competitive distributions such as the moment exponential (MEx) distribution, Haq distribution [35], Xgamma distribution [36], XLindley distribution [37], and Lindley distribution.

The parameters of all considered are estimated using the MLE approach. We utilized the maximum log-likelihood (l), Akaike information criterion (AIC), Bayesian information criterion (BIC), and Kolmogorov-Smirnov goodness-of-fit metrics to explore the fitting performance and selection of the best-fitted model. The MLEs and model selection metrics for both datasets are presented in Tables 9 and 10, respectively.

Table 9: The parameter estimates and goodness-of-fit measures of all fitted distributions for COVID-19 data

Distribution	Estimate (S.E.)	$-l$	AIC	BIC	KS (p-value)	AD (p-value)	CVM (p-value)
SMEx	4.5231 (0.5203)	77.285	156.57	157.97	0.1100 (0.8200)	0.2930 (0.9400)	0.0436 (0.9200)
MEx	3.0782 (0.3974)	78.048	158.10	159.50	0.1430 (0.5200)	0.5340 (0.7100)	0.0843 (0.6700)
Haq	0.3527 (0.0417)	82.336	166.67	168.07	0.2210 (0.0900)	1.8500 (0.1100)	0.3190 (0.1200)
Xgamma	0.4066 (0.0462)	79.991	161.98	163.38	0.1710 (0.3100)	1.0200 (0.3500)	0.1580 (0.3700)

(Continued)

Table 9 **(continued)**

Distribution	Estimate (S.E.)	$-l$	AIC	BIC	KS (p-value)	AD (p-value)	CVM (p-value)
XLindley	0.2631 (0.0347)	81.261	164.52	165.92	0.2020 (0.1500)	1.4600 (0.1900)	0.2420 (0.2000)
Lindely	0.2884 (0.0377)	79.964	161.93	163.33	0.1790 (0.2600)	1.0600 (0.3300)	0.1700 (0.3300)

Table 10: The parameter estimates and goodness-of-fit measures of all fitted distributions for precipitation data

Distribution	Estimate (S.E.)	$-l$	AIC	BIC	KS (p-value)	AD (p-value)	CVM (p-value)
SMEx	1.2405 (0.1428)	38.897	79.794	81.195	0.0773 (0.9900)	0.1710 (1.0000)	0.0208 (1.0000)
MEx	0.8375 (0.1081)	39.239	80.477	81.879	0.1110 (0.8500)	0.3970 (0.8500)	0.0570 (0.8400)
Haq	0.9278 (0.1254)	46.330	94.659	96.060	0.2500 (0.0480)	2.8100 (0.0340)	0.5160 (0.0360)
Xgamma	1.1900 (0.1516)	44.574	91.147	92.548	0.2230 (0.1000)	2.1700 (0.0750)	0.3820 (0.0800)
XLindley	0.7799 (0.1108)	44.548	91.096	92.497	0.2140 (0.1300)	2.0900 (0.0830)	0.3600 (0.0920)
Lindley	0.9096 (0.1247)	43.144	88.287	89.689	0.1880 (0.2400)	1.5900 (0.1600)	0.2620 (0.1700)

6.1 Data Set I

The first dataset is epidemiological data originally analyzed [38]. The dataset is about the mortality rate in the Netherlands due to COVID-19 from 31st March to 30th April 2020. The data observations are given below.

14.918	10.656	12.274	10.289	10.832	7.099	5.928	13.211	7.968	7.584
5.5550	6.0270	4.0970	3.611	4.960	7.498	6.940	5.307	5.048	2.857
2.254	5.431	4.462	3.883	3.461	3.647	1.974	1.273	1.416	4.235

To understand the nature of the COVID-19 dataset, we draw non-parametric plots (Box, Total Time on Test (TTT), violin, and Q-Q) and present them in Fig. 3.

The dataset exhibits a right-skewed behavior, as evidenced by a coefficient of skewness which is 0.83 and visually supported by box and violin plots. The mean of the dataset is 6.16, with a variance of about 12.48, indicating considerable dispersion. The lengthy right tail in both the histogram and the violin plot indicates that most observations are concentrated at lower values, with a few relatively big outliers dragging the distribution to the right. The boxplot demonstrates this skewness, with the median closer to the lower quartile and an outlier at the upper end. The TTT plot shows an increasing failure rate. Overall, the dataset exhibits non-normal, positively skewed behavior, with little inclination towards a heavy-tailed distribution.

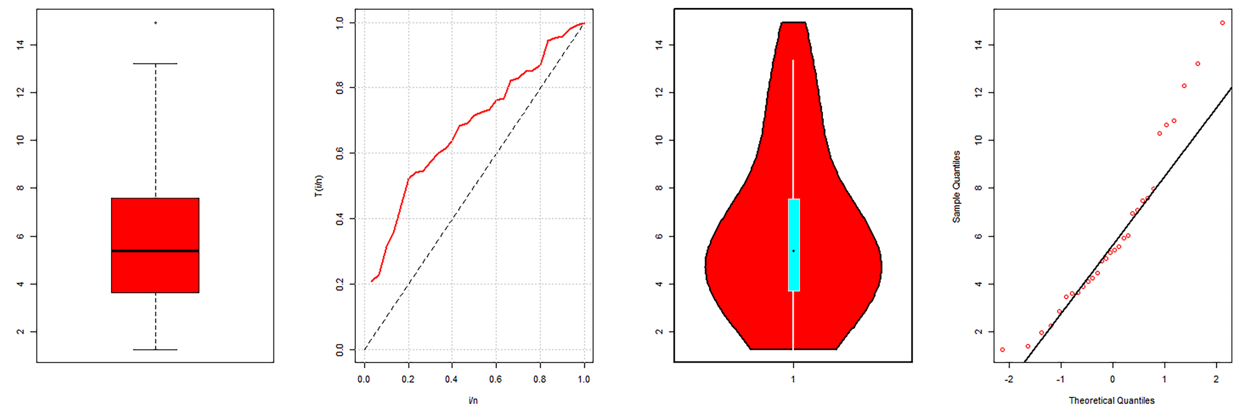

Figure 3: Box, TTT, Violin, and Q-Q plots based on COVID-19 data

6.2 Data Set II

The second dataset presented below pertains to precipitation measured in inches [39]. The data observations are.

0.77	1.74	0.81	1.20	1.95	1.20	0.47	1.43	3.37	2.20	3.00	3.09	1.51	2.10	0.52
1.62	1.31	0.32	0.59	0.81	2.81	1.87	1.18	1.35	4.75	2.48	0.96	1.89	0.90	2.05

To explore the characteristics of the precipitation dataset, we utilize non-parametric plots including Boxplot, Total Time on Test (TTT) plot, violin plot, and Q-Q plot which are presented in Fig. 4.

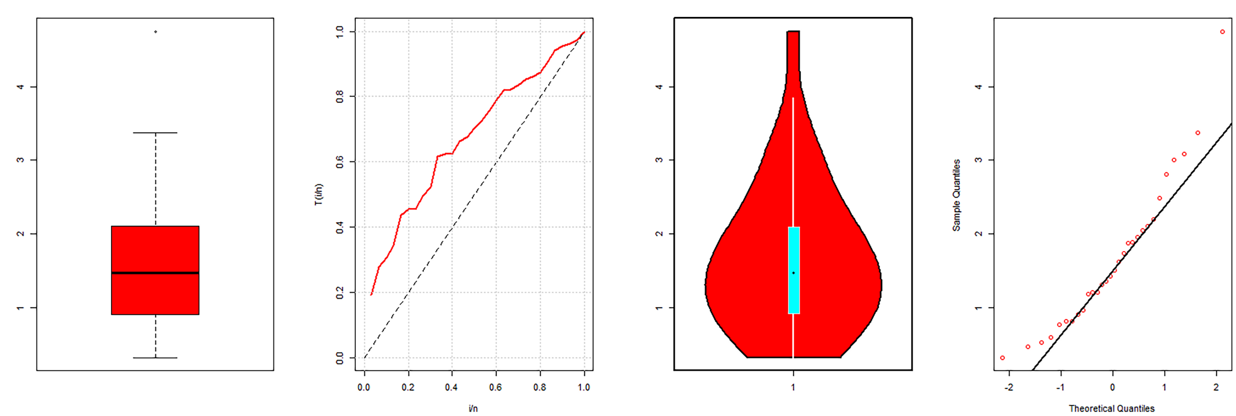

Figure 4: Box, TTT, Violin, and Q-Q plots based on precipitation data

The second dataset reveals a positively skewed distribution with an average of 1.675 and a variance of 1.001. The data is right-tailed, according to the skewness score of 1.087, with a few high precipitation values pushing the distribution to the right. A leptokurtic shape, which has a sharper peak and heavier tails than a normal distribution, is suggested by a kurtosis score of 1.207. Visualizations such as the boxplot and violin plot reflect the data's skewed character, with the bulk of values centered between 1 and 2 inches and an outlier at 4.75 inches. Furthermore, the TTT plot shows an increasing failure rate pattern.

Based on these findings, the SMEx distribution efficiently analyzed both considered datasets as compared to the considered competitive distributions. Figs. 5 and 6 show the estimated PDF, CDF, and hazard function of the SMEx distribution for both datasets.

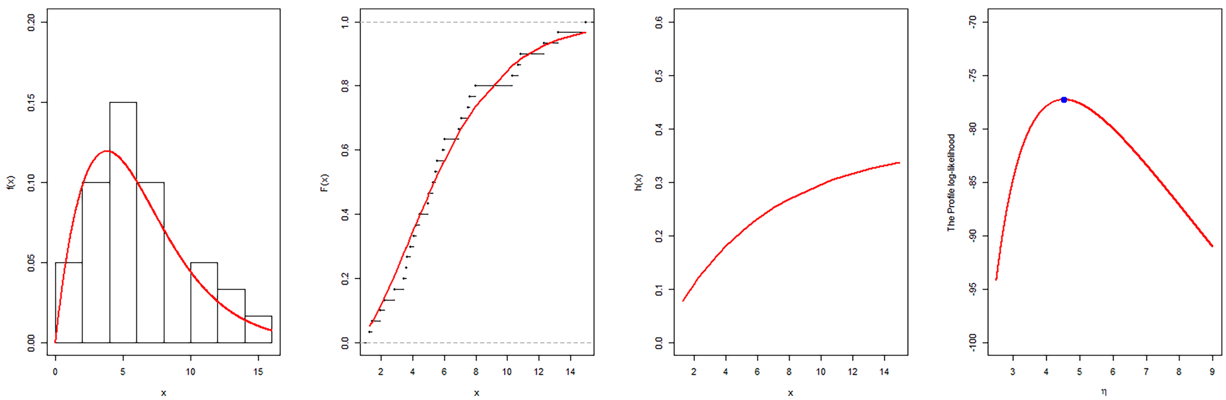

Figure 5: The density, CDF, hazard function, and profile log-likelihood curves of the fitted SMEx distribution to COVID-19 data

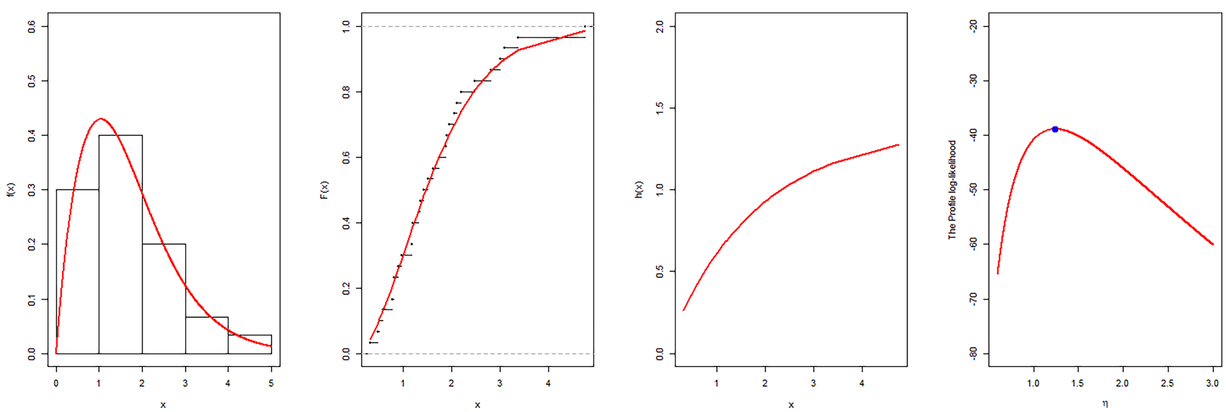

Figure 6: The density, CDF, hazard function, and profile log-likelihood curves of the fitted SMEx distribution to precipitation data

7 Conclusion

In this study, we introduced a new extended distribution. The new model is derived using the Sine-G family of distributions and is named the Sine-Moment Exponential (SMEx) distribution. We have derived various key theoretical characteristics, including quantile function, incomplete moments, complete moments with associated measures, hazard function, mean residual life function, and order statistics. Henceforth, five estimation approaches are used to get the estimation of the SMEx distribution parameter. We performed a detailed Monte Carlo simulation study to explore the estimation performance of these considered estimation methods. In the end, two applications were taken from epidemiological and climatic fields to demonstrate the applicability of the proposed distribution, and it is shown that the SMEx distribution is more efficiently analyzed in both datasets.

8 Future Work

In this study, we introduce a novel model and explore. There are several promising avenues that are still open for future research based on this probability distribution. These future directions not only deepen the theoretical understanding of the model but also expand its applicability across various arenas. The areas for future study include:

- Extending the proposed distribution to handle censored data is another key direction, particularly for the modeling of survival and reliability analysis, where left, right, and interval censoring frequently occur; for more details, see the references [40–43].
- Estimation of the entropy measures, such as Rényi entropy and Shannon entropy, would provide deeper insights into the uncertainty and power of the distribution; for more details, see the references [44–47].
- Another potential development involves extending the baseline distribution using a neutrosophic approach to analyze vague datasets for more detail, see the references [48–51].
- The proposed distribution can be explored for complex and high-dimensional data analysis, particularly in the area of image analysis and feature representations, see the references [52,53].

Acknowledgement: Not applicable.

Funding Statement: The authors received no specific funding for this study.

Author Contributions: The authors confirm contribution to the paper as follows: Hazar A. Khogeer has made the mathematics and programming writing and Amani Alrumayh has made the mathematics and programming writing. All authors reviewed the results and approved the final version of the manuscript.

Availability of Data and Materials: All data exists in the paper with its related references.

Ethics Approval: Not applicable.

Conflicts of Interest: The authors declare no conflicts of interest to report regarding the present study.

References

1. Meraou MA, Al-Kandari NM, Raqab MZ, Kundu D. Analysis of skewed data by using compound Poisson exponential distribution with applications to insurance claims. J Stat Comput Simul. 2022;92(5):928–56. doi:10.1080/00949655.2021.1981324.
2. Meraou MA, Al-Kandari NM, Raqab MZ. Univariate and bivariate compound models based on random sum of variates with application to the insurance losses data. J Stat Theory Pract. 2022;16(4):56. doi:10.1007/s42519-022-00282-8.
3. Gemeay AM, Ezzebsa A, Zeghdoudi H, Tanış C, Tashkandy YA, Bakr ME, et al. The power new XLindley distribution: statistical inference, fuzzy reliability, and applications. Heliyon. 2024;10(17):e36594. doi:10.1016/j.heliyon.2024.e36594.
4. Karakaya K, Taniş C. Estimating the parameters of xgamma weibull distribution. Adıyaman Univ J Sci. 2020;10(2):557–71. doi:10.37094/adyujsci.781069.
5. Bashiru SO, Kayid M, Sayed RM, Balogun OS, Hammad AT, Abd El-Raouf MM. Transmuted inverse unit teissier distribution: properties, estimations and applications to medical and radiation sciences. J Radiat Res Appl Sci. 2025;18(1):101208. doi:10.1016/j.jrras.2024.101208.

6. Sapkota LP, Kumar V, Tekle G, Alrweili H, Mustafa MS, Yusuf M. Fitting real data sets by a new version of gompertz distribution. Mod J Stat. 2025;1(1):25–48. doi:10.64389/mjs.2025.01109.
7. Noori NA, Abdullah KN, Khaleel MA. Development and applications of a new hybrid weibull-inverse weibull distribution. Mod J Stat. 2025;1(1):80–103. doi:10.64389/mjs.2025.01112.
8. Bashiru SO. A study on the properties of a new exponentiated extended inverse exponential distribution with applications. Reliab Theory Appl. 2023;18(3(74)):59–72.
9. Shaw WT, Buckley IR. The alchemy of probability distributions: beyond gram-charlier & cornish-fisher expansions, and skew-normal or kurtotic-normal distributions. Submitt. 2007;7:64.
10. Eugene N, Lee C, Famoye F. Beta-normal distribution and its applications. Commun Stat Theory Meth. 1995;31:497–512. doi:10.1081/STA-120003130.
11. Bourguignon M, Silva RB, Cordeiro GM. The weibull-G family of probability distributions. J Data Sci. 2014;12(1):53–68. doi:10.6339/jds.201401_12(1).0004.
12. Kumar D, Singh U, Singh SK. A new distribution using sine function-its application to bladder cancer patients data. J Stat Appl Probab. 2015;4(3):417.
13. Ul Haq MA, Elgarhy M. The odd Frechet-G family of probability distributions. J Stat Appl Pro. 2018;7(1):189–203. doi:10.18576/jsap/070117.
14. Hassan AS, Nassr SG. Power Lindley-G family of distributions. Ann Data Sci. 2019;6(2):189–210. doi:10.1007/s40745-018-0159-y.
15. Al-Babtain AA, Elbatal I, Al-Mofleh H, Gemeay AM, Afify AZ, Sarg AM. The flexible burr X-G family: properties, inference, and applications in engineering science. Symmetry. 2021;13(3):474. doi:10.3390/sym13030474.
16. Alkhairy I, Nagy M, Muse AH, Hussam E. The arctan-X family of distributions: properties, simulation, and applications to actuarial sciences. Complexity. 2021;2021:4689010. doi:10.1155/2021/4689010.
17. Eghwerido JT, Nzei LC, Omotoye AE, Agu FI. The teissier-G family of distributions: properties and applications. Math Slovaca. 2022;72(5):1301–18. doi:10.1515/ms-2022-0089.
18. Rajkumar J, Sakthivel KM. A new method of generating Marshall-olkin sine-G family and its applications in survival analysis. Lobachevskii J Math. 2022;43(2):463–72. doi:10.1134/s1995080222050213.
19. Nanga S, Nasiru S, Dioggban J. Cosine topp-leone family of distributions: properties and regression. Res Math. 2023;10:2208935. doi:10.1080/27684830.2023.2208935.
20. Al Abbasi JN, Afify AZ, Alnssyan B, Shama MS. The lambert-G family: properties, inference, and applications. Comput Model Eng Sci. 2024;140(1):513–36. doi:10.32604/cmes.2024.046533.
21. Hussam E, Sapkota LP, Gemeay AM. Tangent exponential-G family of distributions with applications in medical and engineering. Alex Eng J. 2024;105:181–203. doi:10.1016/j.aej.2024.06.034.
22. Ahmad A, Rather AA, Gemeay AM, Nagy M, Sapkota LP, Mansi AH. Novel sin-G class of distributions with an illustration of Lomax distribution: properties and data analysis. AIP Adv. 2024;14(3):035132. doi:10.1063/5.0180263.
23. El-Sherpieny EA, Almetwally EM, Muhammed HZ. Bivariate weibull-G family based on Copula function: properties, Bayesian and non-Bayesian estimation and applications. Stat Optim Inf Comput. 2022;10(3):678–709. doi:10.19139/soic-2310-5070-1129.
24. Atchadé MN, Agbahide AA, Otodji T, Bogninou MJ, Moussa Djibril A. A new shifted Lomax-X family of distributions: properties and applications to actuarial and financial data. Comput J Math Stat Sci. 2025;4(1):41–71. doi:10.21608/cjmss.2024.307114.1066.
25. Husain QN, Qaddoori AS, Noori NA, Abdullah KN, Suleiman AA, Balogun OS. New expansion of Chen distribution according to the nitrosophic logic using the gompertz family. Innov Stat Prob. 2025;1(1):60–75. doi:10.64389/isp.2025.01105.
26. ElSherpieny EA, Almetwally EM. The exponentiated generalized alpha power family of distribution: properties and applications. Pak J Stat Oper Res. 2022;18(2):349–67. doi:10.18187/pjsor.v18i2.3515.

27. Osi AA, Abdalla GSS, Sawaran Singh NS, Suleiman AA. Advancing lifetime data modeling via the Marshall-Olkin cosine Topp-Leone distribution family. Comput J Math Stat Sci. 2025;4(2):476–99. doi:10.21608/cjmss.2025.374786.1155.
28. Bashiru SO, Isa AM, Khalaf AA, Khaleel MA, Arum KC, Anioke CL. A hybrid cosine inverse Lomax-G family of distributions with applications in medical and engineering data. Niger J Technol Dev. 2025;22(1):261–78.
29. Dara ST, Ahmad M. Recent advances in moment distribution and their hazard rates. Cham, Switzerland: LAP LAMBERT Academic Publishing; 2012.
30. Haq MAU, Hashmi S, Aidi K, Ramos PL, Louzada F. Unit modified burr-III distribution: estimation, characterizations and validation test. Ann Data Sci. 2023;10(2):415–40. doi:10.1007/s40745-020-00298-6.
31. Ahsan-ul-Haq M, Memon AZ, Chand S. An analysis of generalized exponential uniform distribution. Math Probl Eng. 2022;2022:6040943. doi:10.1155/2022/6040943.
32. Alomair AM, Ahmed M, Tariq S, Ahsan-Ul-Haq M, Talib J. An exponentiated XLindley distribution with properties, inference and applications. Heliyon. 2024;10(3):e25472. doi:10.1016/j.heliyon.2024.e25472.
33. Hassan AS, Metwally DS, Elgarhy M, Gemeay AM. A new probability continuous distribution with different estimation methods and application. Comput J Math Stat Sci. 2025;4(2):512–32. doi:10.21608/cjmss.2025.375970.1157.
34. Alzahrani MR, Almohaimeed M. Analysis, inference, and application of Unit Haq distribution to engineering data. Alex Eng J. 2025;117:193–204. doi:10.1016/j.aej.2025.01.050.
35. Ahsan-Ul-Haq M. Statistical analysis of Haq distribution: estimation and applications. Pakistan J Stat. 2022;38(4):473–90.
36. Sen S, Maiti SS, Chandra N. The xgamma distribution: statistical properties and application. J Mod App Stat Meth. 2016;15(1):774–88. doi:10.22237/jmasm/1462077420.
37. Chouia S, Zeghdoudi H. The XLindley distribution: properties and application. J Stat Theory Appl. 2021;20(2):318–27. doi:10.2991/jsta.d.210607.001.
38. Almongy HM, Almetwally EM, Aljohani HM, Alghamdi AS, Hafez EH. A new extended Rayleigh distribution with applications of COVID-19 data. Results Phys. 2021;23:104012. doi:10.1016/j.rinp.2021.104012.
39. Hinkley D. On quick choice of power transformation. J R Stat Soc Ser C. 1997;26:67–9. doi:10.2307/2346869.
40. Qayoom D, Rather AA, Alsadat N, Hussam E, Gemeay AM. A new class of Lindley distribution: system reliability, simulation and applications. Heliyon. 2024;10(19):e38335. doi:10.1016/j.heliyon.2024.e38335.
41. Sabry MAH, Almetwally EM, Alamri OA, Yusuf M, Almongy HM, Eldeeb AS, et al. Inference of fuzzy reliability model for inverse Rayleigh distribution. AIMS Math. 2021;6(9):9770–85. doi:10.3934/math.2021568.
42. El Gazar AM, Ramadan DA, ElGarhy M, El-Desouky BS. Estimation of parameters for inverse power ailamujia and truncated inverse power ailamujia distributions based on progressive type-II censoring scheme. Innov Stat and Prob. 2025;1(1):76–87. doi:10.64389/isp.2025.01106.
43. Meraou MA, Al-Kandari NM, Mohammad RZ. Fundamental properties of the characteristic function using the compound Poisson distribution as the sum of the gamma model. Mod J Stat. 2025;1(1):49–57. doi:10.64389/mjs.2025.01110.
44. Chidzalo P, Abonongo J, Naryongo R. Enhancing reliability and accuracy in stochastic growth modeling: method of three selected points approach. Comput J Math Stat Sci. 2023;2(2):291–302. doi:10.21608/cjmss.2023.240689.1021.
45. Ramses El-Saeed A, Abdellatif AD. Point and interval estimation of reliability and entropy for generalized exponential distribution under generalized type-II hybrid censoring scheme. Comput J Math Stat Sci. 2025;4(1):96–138. doi:10.21608/cjmss.2024.327558.1078.

46. Afify AZ, Gemeay AM, Alfaer NM, Cordeiro GM, Hafez EH. Power-modified kies-exponential distribution: properties, classical and Bayesian inference with an application to engineering data. Entropy. 2022;24(7):883. doi:10.3390/e24070883.
47. Ahsan Ul Haq M, Aslam M. Comparison of entropy measures for gompertz and truncated gompertz distribution. Proc Natl Acad Sci Ind Sect A Phys Sci. 2023;93(1):113–20. doi:10.1007/s40010-022-00797-6.
48. Albassam M, Ahsan-Ul-Haq M, Aslam M. Weibull distribution under indeterminacy with applications. AIMS Math. 2023;8(5):10745–57. doi:10.3934/math.2023545.
49. Ahsan-Ul-Haq M. A new Cramèr-von mises goodness-of-fit test under uncertainty. Neutrosophic Sets Syst. 2022;49:262–8.
50. Ahsan-Ul-Haq M. Neutrosophic kumaraswamy distribution with engineering application. Neutrosophic Sets Syst. 2022;49:269–76.
51. Khan Z, Gulistan M, Kausar N, Park C. Neutrosophic Rayleigh model with some basic characteristics and engineering applications. IEEE Access. 2021;9:71277–83. doi:10.1109/access.2021.3078150.
52. Liu Y, Wang C, Lu M, Yang J, Gui J, Zhang S. From simple to complex scenes: learning robust feature representations for accurate human parsing. IEEE Trans Pattern Anal Mach Intell. 2024;46(8):5449–62. doi:10.1109/TPAMI.2024.3366769.
53. Wang C, Zhang Q, Wang X, Zhou L, Li Q, Xia Z, et al. Light-field image multiple reversible robust watermarking against geometric attacks. IEEE Trans Dependable Secure Comput. 2025;22(6):5861–75. doi:10.1109/TDSC.2025.3576223.